

## NOISE REDUCTION TECHNIQUES FOR ELECTRONIC SPECKLE INTERFEROMETRY

Bruno Pouet  
Sridhar Krishnaswamy  
Center for Quality Engineering and Failure Prevention  
Northwestern University  
Evanston, IL 60208

### INTRODUCTION

Video-based speckle interferometric methods such as electronic speckle pattern interferometry (ESPI) allow us to measure full-field surface deformation of a diffuse object. In this paper we show, in a first step, that the susceptibility of ESPI to noise can be substantially reduced [1] by synchronizing the optical interferometer and the object stressing system with the CCD image acquisition and processing system, and by performing what amounts to a repetitive sequence of rapid ESPI tests. In this manner, a stable fringe pattern can be obtained as long as the ambient noise is of sufficiently lower frequency than the video acquisition rate (typically 30 Hz). This scheme will be referred in this paper as reference-updating subtractive correlated ESPI to distinguish it from classical ESPI. We then take this issue further with a hybrid additive-subtractive decorrelated ESPI technique that will freeze out unwanted environmental noise of frequencies much higher than video rates [2]. The basic principle of this proposed technique can be summed up as follows: (i) acquire speckle images containing information about the same two deformed object states in every frame of the image acquisition sequence, (ii) decorrelate the speckles between every frame, and (iii) compare every consecutive pair of speckle images to extract visible fringes corresponding to the two deformed states of the test object.

All three ESPI techniques are comparatively assayed using a flat-bottomed hole specimen that is acoustically resonated. Additionally, adhesively bonded specimens are investigated for disbonds, showing the practical application of the proposed methods in NDE.

### PRINCIPLE AND THEORETICAL DESCRIPTION

A schematic of the ESPI setup is shown in Fig. 1. A coherent laser beam is passed through an acousto-optic modulator which is used as an optical shutter. The laser beam is split by means of a beam splitter into two legs each of which is expanded by beam expanders. One of the expanded beams is used as the reference beam by passing it through a ground glass diffuser. The other beam is used to illuminate the test object that is acoustically stressed using piezoelectric transducers. A speckle pattern produced by the coherent light scattered from a diffuse test object (object beam) is made to interfere with the reference beam,

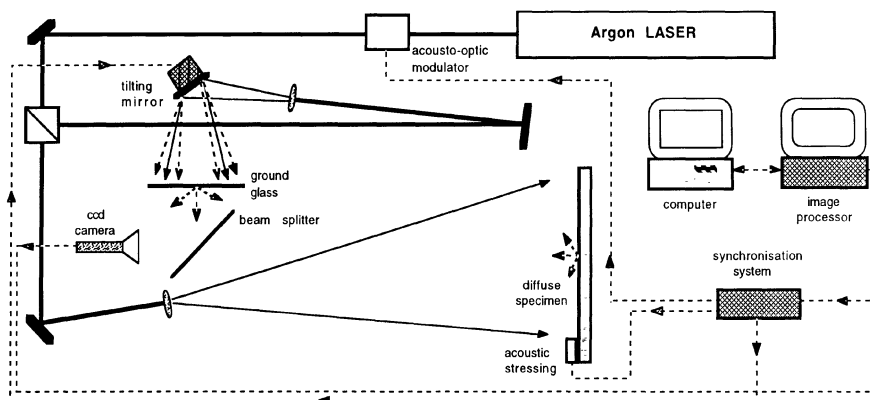


Fig. 1 Schematic of the experiment.

and the resulting interference speckle pattern is collected into a CCD camera for recording by a digital image processing computer system. This recorded speckle pattern carries information corresponding to the surface topology of the test object. If a second speckle pattern is then recorded with a slightly different surface shape for the object (here caused by acoustically stressing the object), it is possible to compare the pair of recorded interference speckle patterns to extract information in the form of a fringe pattern corresponding to the relative object deformation. The desired information about the relative object deformation can be extracted from the pair of recorded speckle patterns by a variety of processing methods including analog and digital signal processing techniques [3,4].

Since the CCD camera integrates the intensity of light impinging on it over the duration of a frame, the intensity recorded by the CCD camera during the recording time  $T$  of the  $N$ th frame may be expressed as:

$$I_N(x) = A_R^2(x) + A_O^2(x) + 2A_R(x)A_O(x) \frac{1}{T} \int_0^T \epsilon_N(t) \cos \{ \phi_S(x,t) \} dt \quad (1)$$

Here  $\epsilon_N(t)$  is an optical shuttering function of the acousto-optic modulator. The quantity ' $t$ ' represents time measured from the start of a CCD frame (that is, it is reinitialized to zero at the beginning of every frame). The reference and object beam amplitudes are denoted by  $A_R(x)$  and  $A_O(x)$  which are assumed to be essentially time-invariant. The speckle phase quantity  $\phi_S(x,t)$  is given by:

$$\phi_S(x,t) = \phi_O(x;N) - \phi_R(x;N) + M(x) \sin \omega t = \phi(x;N) + M(x) \sin \omega t \quad (2)$$

and represents the difference in the phases of the reference and object beams. It consists of a random speckle phase component denoted for simplicity by  $\phi(x;N)$ ; and a part which represents the signal of interest where  $M(x)$  is the corresponding amplitude of the displacement-induced phase, and  $\omega$  is the frequency of the acoustic stressing. Information about the relative object displacement can thus be extracted by subtracting two speckle images corresponding to say the  $N_0^{\text{th}}$  and  $N_1^{\text{th}}$  frames. That is, "brightness"  $q(x, N_0, N_1) = |I_{N_1} - I_{N_0}|$ , is computed and displayed on a monitor in real-time. By using different optical shutter functions in expression (1), it is possible to obtain a variety of modulations leading to real-time or time-averaged information [5]. For simplicity we will derive the expression corresponding only to the case of real-time modulation, wherein the acousto-optic modulator is pulsed in phase with the extrema of the acoustic stressing. A similar analysis will hold for other types of modulations. The timing sequences corresponding to the real time modulation for the different ESPI techniques discussed in this paper are shown Figure 2.

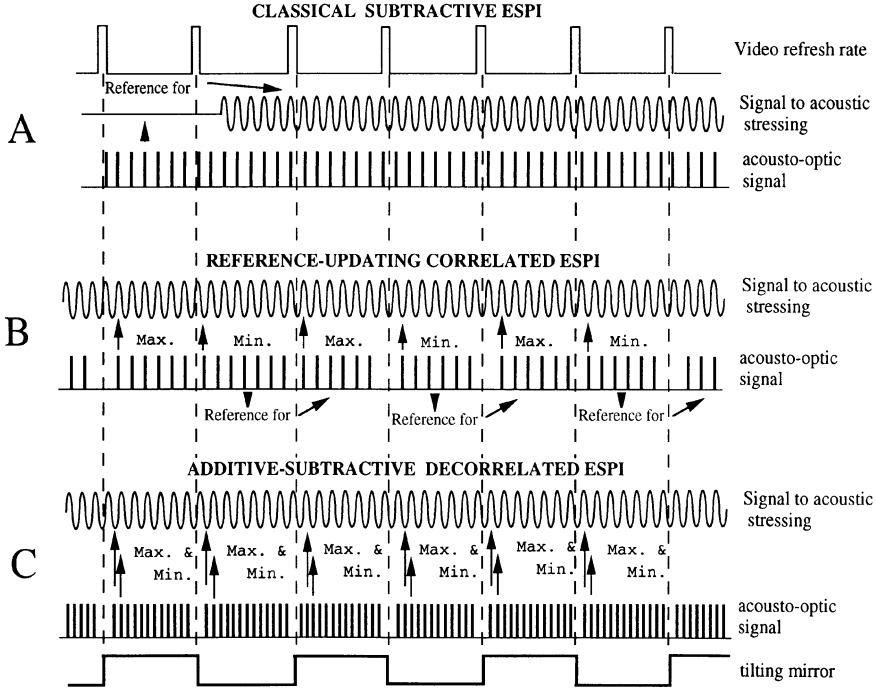


Fig. 2 Timing sequence for real-time modulation for: A - Classical subtractive ESPI, B - Reference-updating correlated ESPI, C - Additive-subtractive decorrelated ESPI.

#### Classical Subtractive ESPI

In classical ESPI, the reference frame is acquired at the beginning of a test when the specimen is at rest, and the current frames corresponding to the acoustically stressed specimen are then subtracted from this original reference. This is achieved through the shutter function (see Fig. 2 a) given by:

$$\epsilon_N(t) = \sum_{k=0}^{k_{\max}} \delta[t - (2k+1/2)\Pi/\omega] \quad (3)$$

where  $k_{\max}$  is the number of pulses that are accommodated within each CCD frame. In this case the brightness can be expressed as:

$$q(x; N_1; N_0) = 4|A_R(x)A_O(x)\sin\{\varphi(x,N)+M(x)/2\}\sin\{M(x)/2\}| \quad (4)$$

This expression is valid only if the speckle phase remains constant during the experiment and no decorrelation occurs. It is clear that in an industrial environment where thermal noise and slow object drift are present, the assumption that the speckle patterns stay correlated will be increasingly violated as the time between the current image and the acquired reference image becomes large. It is for this reason that the fringe stability and contrast degrades with time in conventional ESPI, requiring that a new reference image be acquired before the test can be resumed.

#### Reference-Updating Subtractive Correlated ESPI

To mitigate the noise susceptibility of classical ESPI, we have recently developed a continual

reference-updating subtractive correlated ESPI technique. In this case, the reference frame is always the one immediately preceding the current one (i.e.,  $N_0 = N_1 - 1$ ). This is done repetitively for any pair of frames in the sequence. In order that different object deformation states will be recorded on consecutive frames, the optical shutter is used to create stroboscopic pulses aligned in phase with the maximum of the acoustic deformation during one CCD frame, and the minimum deformation during the next; see Fig. 2 b. This is achieved through the shutter function for frames  $N_0$  and  $N_1$  given by:

$$\epsilon_{N_0}(t) = \sum_{k=0}^{k_{\max}} \delta[t - (2k+1/2)\Pi/\omega] \quad \text{and} \quad \epsilon_{N_1}(t) = \sum_{k=0}^{k_{\max}} \delta[t - (2k+3/2)\Pi/\omega], \quad (5)$$

The brightness therefore becomes:

$$q(x; N_1; N_0) = 4|A_R(x)A_O(x)| \sin\{\varphi(x, N)\} \sin\{M(x)\} \quad (6)$$

This relation shows that this technique is more sensitive than its counterpart in conventional ESPI because in this case the differential deformation is twice as large as in the classical technique. Also, since every consecutive pair of frames is compared, decorrelation causing noise of frequencies sufficiently lower than video rates are frozen out. However, as with the classical ESPI, expression (6) is valid only if the speckle pattern is correlated for the two subtracted images, which means that the speckle patterns stay stable during two consecutive images (for 60 ms with the standard CCD acquisition rate). When the noise frequency is high enough that speckle phase cannot remain constant during two frames, an alternate procedure must be used in order to obtain meaningful fringe patterns despite the noise.

#### Additive-Subtractive Decorrelated ESPI

In this case, speckle patterns from the same set of two different deformed object states are added together in every frame of the CCD acquisition sequence. This is achieved by use of the following optical shutter function which is the same for every frame:

$$\epsilon_{N_0}(t) = \epsilon_{N_1}(t) = \sum_{k=0}^{k_{\max}} \{\delta[t - (2k+1/2)\Pi/\omega] + \delta[t - (2k+3/2)\Pi/\omega]\}. \quad (7)$$

Thus, there are two pulses of illumination in every cycle of vibration of the object, and these are aligned with the two extrema positions as shown in Fig. 2 c. In addition, a tilting mirror is used to intentionally decorrelate the speckles between each frame. Using the fact that the average intensity is constant from frame to frame, the brightness becomes:

$$q(x; N_1; N_0) = 4|A_O(x)A_R(x)| |\cos\{\varphi(x; N_1)\} - \cos\{\varphi(x; N_0)\}| |\cos\{M(x)\}|, \quad (8)$$

where the random speckle phase in frame  $N_1$  is decorrelated with respect to that of frame  $N_0$  (i.e.  $\varphi(x, N_0) \neq \varphi(x, N_1)$ ). In this case the fringe pattern is described by absolute-cosine fringes as in additive ESPI. The main advantage with this technique is that, thanks to the additive process during each frame, the fringe pattern is very robust even in noisy environment [2]. In this case, the loss of fringes caused by noise decorrelation appears only at frequencies close to the frequency of the acoustic stressing, and not at frequencies corresponding to the CCD acquisition rate as with the reference-updating ESPI.

## RESULTS AND APPLICATION TO NDE OF DISBONDS

Experiments were performed using the three methods of ESPI described above with the set-up shown in Fig. 1. The first specimen used in the investigation was an aluminum plate (1 x 10 x 12 inches) with a flat-bottomed hole 3 inch in diameter leaving a 1/32 inch thick membrane located at the center of the plate. Because of the difference in thickness between the membrane portion and the surrounding plate, the resonant frequencies

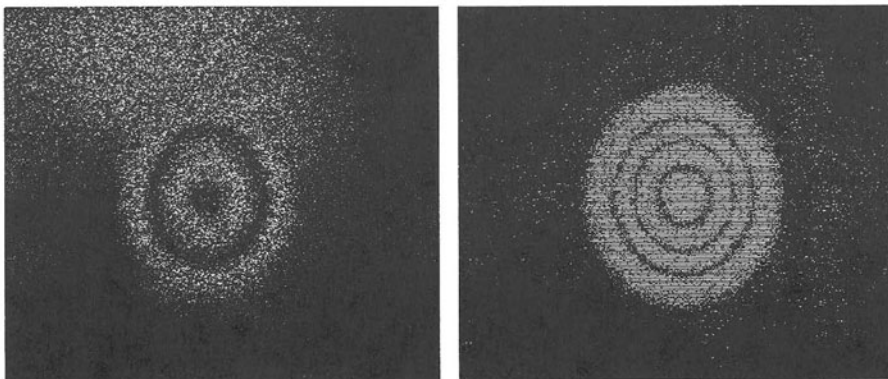


Fig. 3 Real-time ESPI recording of a flat-bottomed hole vibrating at 1.37 kHz:  
A: Classical subtractive ESPI; B: reference-updating correlated ESPI.

corresponding to the flat-bottomed hole were completely different from those of the overall plate modes. This allowed us to investigate the resonance of the flat-bottomed hole without any identification problems arising from possible superposition of unwanted plate mode vibrations of the entire specimen.

Figure 3 shows the results of experiments done in a quiet laboratory environment. The results correspond to specimen vibration at a resonant frequency of 1.37kHz for the classical and the reference-updating ESPI techniques. The experimental circumstances (acoustic stressing level, etc.) were kept the same for all the experiments in each comparison set. As we can see, the image quality is better with the reference-updating technique. The noise that leads to speckle decorrelation and the consequent contrast reduction associated with the conventional technique are eliminated. In like manner, figures 4 a and 4 b show the comparison between reference-updating subtractive correlated ESPI and additive-subtractive decorrelated ESPI for a resonant frequency of 31kHz. As expected, the two images are complementary: absolute-sine fringes with subtractive correlated ESPI, and absolute-cosine fringes with additive-subtractive decorrelated ESPI. It must be noted that although the environment was relatively quiet, some amount of noise is still present and is visible in the subtractive correlated ESPI fringes as can be seen from the speckle noise in regions where a black fringe is expected. In the figures 4 c and 4 d ambient noise was extraneously artificially introduced. The experiment was realized with thermal currents induced by a heater placed between the CCD camera and the test specimen. As we can see with the subtractive correlated ESPI method, the fringe contrast is very poor and the fringes become invisible in places where the noise decorrelation is too large. On the other hand, with the additive-subtractive decorrelated ESPI technique, the fringes are still sufficiently visible. It must be noted, the thermal currents are visible as a modulation of the speckle superimposed on the surface displacement fringes but the dark fringes corresponding to the acoustic stressing remain stable, while the thermally induced noise is not.

Next, the two proposed ESPI techniques were applied to NDE of disbonds. Two disbond specimens were built as shown in Fig. 5. The two specimens were two layer aluminum composite plates with a thick back plate (1/2 inch thick) and a thin front plate (1/32 inch thick) bonded together using an epoxy adhesive. Three artificial disbonds in the first specimen (three circular disbonds of 3, 2 and 1 inches in diameter) and seven artificial disbonds in the second specimen (four circular disbonds of 3, 2, 1, and 1/2 inches in diameter, and a square, a triangular and an elliptic disbond) were introduced into the bonding layer by placing thin sheets of teflon between the two plates prior to bonding. The result corresponding to the disbond specimen #1 is given in Fig. 6. Figures 6 a-c. show the fringe patterns corresponding to the resonance of each disbond, obtained with reference-updating subtractive correlated ESPI. Here the CCD camera was focused on each disbond in order to better resolve the fringes. The resonance frequencies of the disbond depend on the disbond size (larger disbond diameters resonate at lower frequencies, for fixed plate

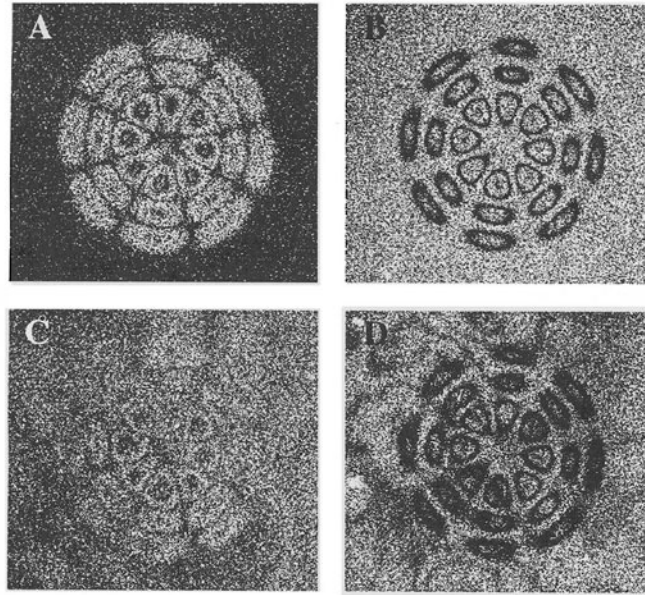


Fig. 4 Comparison between reference-updating subtractive correlated ESPI (A and C) and additive-subtractive decorrelated ESPI (B and D) for the flat-bottomed hole specimen vibrating at 31kHz.

thickness). The stressing frequency used for each disbond did not correspond to the first resonant mode, but rather to a higher mode. The unsymmetric nature of some of the fringe patterns originates from experimental parameters which can not be completely controlled during the fabrication process. Figure 6 d shows an overview of the plate under high frequency acoustic stressing. In this picture the three disbands are visible simultaneously. The frequency used corresponds to forced excitation of the three disbands but not to the maximum/ideal resonance for each disbond. At the same time, it is also possible to see some fringes corresponding to the vibration-induced deformation of the entire thin ply of the two-ply sandwich plate. Finally, the results for disbond specimen #2 are shown in Fig. 7 for

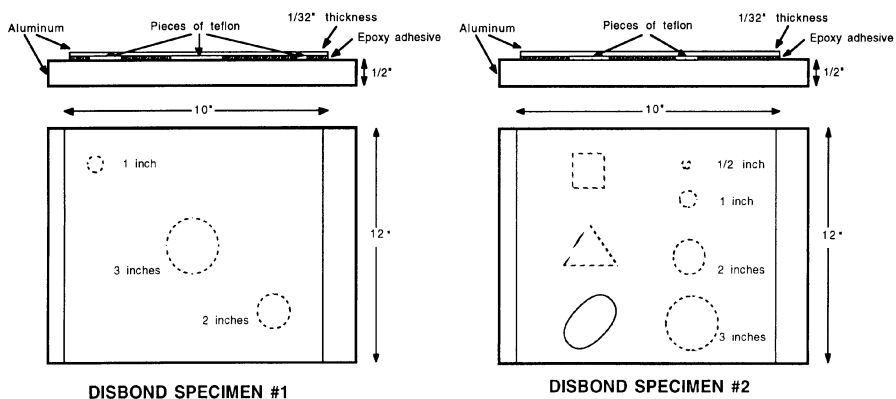


Fig. 5 Disbond specimen geometries.

disbond forcing frequency of 44 kHz. With the additive-subtractive decorrelated ESPI method, the four circular disbonds (1/2, 1, 2 and 3 inch of diameter) and the square, elliptic and triangle disbonds are all visible without ambiguity. For the same experimental circumstances, using the subtractive correlated ESPI technique, the square disbond as well as the 1/2 and 1 inch circular disbonds are obscured by ambient noise. As can be seen from Fig.7, the proposed additive-subtractive decorrelated technique clearly appears to be a better tool than conventional or reference-updating subtractive correlated ESPI techniques, especially from an NDE standpoint where fringe stability is an important issue in terms of increasing the probability of defect detection by the operator.

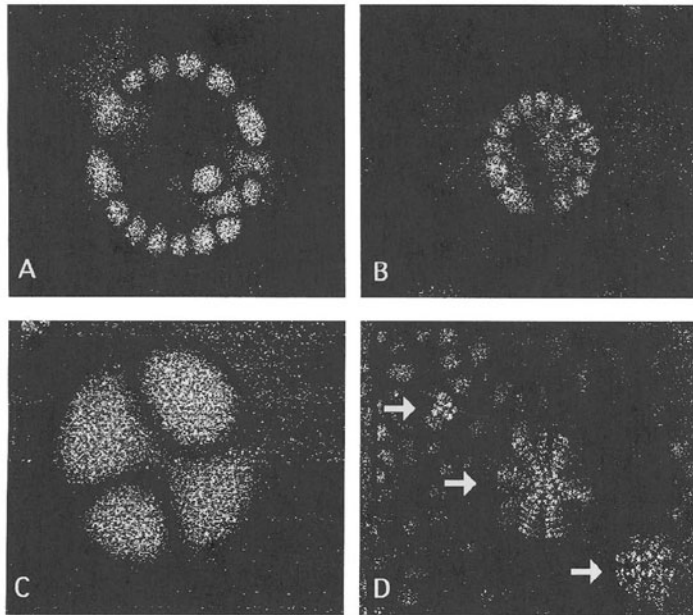


Fig. 6 Reference-updating correlated ESPI used on disbond specimen #1. A: 3 inch disbond, resonant frequency 18kHz, B: 2 inch disbond, resonant frequency 26 kHz, C: 1 inch disbond, resonant frequency 29kHz, D: plate overview, forcing frequency 65kHz.

## CONCLUSION

Modifications to the classical subtractive ESPI technique are proposed as a way to minimize the susceptibility of optical NDE methods to environmental noise. Two methods -- reference updating subtractive correlated ESPI and additive-subtractive decorrelated ESPI -- are described. It is shown that additive-subtractive decorrelated ESPI significantly improves fringe stability and contrast in comparison with reference-updating subtractive correlated ESPI, which in turn is an improvement over the classical subtractive ESPI method.

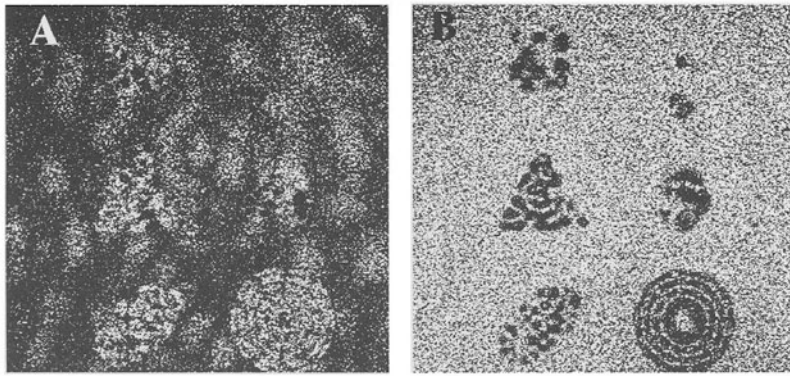


Fig. 7 Disbond specimen #2 vibrating at a forcing frequency of 44 KHz showing various disbonds: A: subtractive correlated ESPI; B: additive-subtractive decorrelated ESPI.

#### ACKNOWLEDGMENT

This work was carried out at Northwestern University in the course of research sponsored by the FAA Center for Aviation Systems Reliability, operated by Ames Laboratory, USDOE, for the Federal Aviation Administration under Contract No. W-7405-ENG-82 for work at Iowa State University.

#### REFERENCES

1. B.F. Pouet, T.C. Chatters and S. Krishnaswamy, submitted to the Journal of Nondestructive Testing (1992).
2. B.F. Pouet and S. Krishnaswamy, submitted to Optical Engineering (1992).
3. K. Creath and G.A. Slettemoen, Journal of the Optical Society of America A, 2, No. 2, p. 1629.(1985).
4. R. Jones and C. Wykes, *Holography and speckle interferometry*, Cambridge University Press (1983).
5. C.C. Aleksoff, in *Holographic Nondestructive Testing*, R. K. Erf(ed), Academic Press, New York, p. 247 (1974).